Proceedings of the 2009 IEEE
International Conference on Robotics and Biomimetics
December 19 -23, 2009, Guilin, China

Modeling and Control of a 7DOF Exoskeleton Robot for Arm Movements

Mohammad H. Rahman, Maarouf Saad*, Jean P. Kenné, and Philippe S. Archambault
*Senior Member, IEEE

Abstract— **To assist a large number of physically disabled people who no longer are in full possession of their body motion, we have been developing an exoskeleton robot *(ExoRob)* to rehabilitate and to ease upper limb motion since movement of shoulder, elbow, and wrist play a vital role in the performance of essential daily activities. The proposed *ExoRob* will be comprised of seven degrees of freedom to enable naturalistic movements of the human upper-limb. This paper focuses on the modeling and control of the proposed *ExoRob*. A kinematical model of *ExoRob* has been developed based on modified Denavit-Hartenberg notations. To achieve the dynamic simulation of the developed model, a nonlinear computed torque control technique is employed. In the simulation, the trajectory tracking performance of the controller is evaluated with the developed dynamic model. Simulation results show that the controller is able to drive the *ExoRob* efficiently to track the desired trajectories, which in this case consisted in passive arm movements. Such movements are used in therapy and could be performed efficiently with the developed model and the controller. This paper also focused on the development of a 7DOF upper-limb prototype (lower scaled) *master exoskeleton arm (mExoArm)* which corresponds to the proposed *ExoRob*. The developed *mExoArm* will be used to maneuver the proposed *ExoRob* (in manual control mode) especially to provide '*passive mode of rehabilitation*'.**

Keywords—Exoskeleton robot (ExoRob), dynamic model, physical disability, rehabilitation, computed torque control, master exoskeleton arm (mExoArm)

I. INTRODUCTION

PHYSICAL disabilities such as full or partial loss of function in the shoulder, elbow or wrist is a common impairment in the *elderly,* but can also be a secondary effect due to *strokes,* trauma, sports injuries, occupational injuries, and spinal cord injuries. Through the last decades the number of disabled people has increased at an alarming rate. Further, studies have shown that a majority of disabled people are senior citizens. Recent statistics among G8 nations reveals that, 13.5% [2] of the total population in Canada are aged 65 and over compared with 21.0% in Japan, 19.9% in Italy, 19.8% in Germany, 16.2% in France, 15.8% in United Kingdom, 14.4% in Russia and 12.6% in the United States [1]. In addition to geriatric disorders, the other major cause of disabilities is stroke. Stroke remains an important cause for morbidity and mortality, and the most common cause for disability. World Health Organization reports reveal that annually more than 20.5 million people worldwide suffer a stroke and cardiovascular diseases, among which 85% of stroke patients incur acute arm impairment, and 40% of victims are chronically impaired or permanently disabled, placing a burden on the family and community. Rehabilitation programs are the main method to promote functional recovery in these subjects. Since the number of such cases is constantly growing and that the duration of treatment is long, exoskeleton robots could significantly contribute to the success of these programs.

To assist such physically disabled people with impaired upper limb function, extensive research has been carried out, in many branches of robotics, particularly exoskeletons [5]-[14]. Although much progress has been made, we are still far from the desired goal, as exoskeleton robots have not lived up to their original promise of restoring body functioning of motion. This is due to limitations in the area of proper hardware design and also of control algorithms to develop autonomous robots to perform intelligent tasks. To develop an exoskeleton robot, the kinematical and dynamic modeling of the robot should resemble to that of the human upper-limb. It is very much important for this kind of robotic system. As a first step toward to develop a seven degrees-of-freedom (7DOF) exoskeleton robot, in this paper we have developed the kinematical and dynamic model of an exoskeleton robot considering upper-limb articulations and movement. Modified Denavit-Hertenberg conventions are used in developing the kinematical model. In dynamic modeling and simulation, robot parameters such as robot arm link lengths, masses, and inertia, are estimated according to the upper limb properties of a typical adult [15], [16]. The nonlinear computed torque control technique [22] is employed in the dynamic simulation of the developed model, with the assumption that control of arm movement is nonlinear in nature. Trajectory tracking performance of the controller is evaluated by comparing the measured trajectories with the desired trajectories. Note that typical upper-limb rehabilitation exercises are considered in generating desired trajectories to simulate the dynamic parameters. The desired trajectories are tracked in validating

Manuscript received July 30 2009.

M. H. Rahman is (Ph.D student) with the Electrical Engineering Department, École De Technologie Superieure, 1100 Notre-Dame, Montreal, Canada, on deputation from Khulna University of Engineering and Technology, Khulna 920300, Bangladesh (e-mail: mohammad-habibur.rahman.1@ens.etsmtl.ca).

M. Saad is with the Electrical Engineering Department, École De Technologie Superieure, 1100 Notre-Dame, Montreal, Canada (phone: 1-514-396-8940; fax: 514-396-8684; e-mail: maarouf.saad@etsmtl.ca).

J.P. Keneé is with the Mechanical Engineering Department, École De Technologie Superieure, 1100 Notre-Dame, Montreal, Canada (e-mail: jean-pierre.kenné @etsmtl.ca).

P. Archambault is with the School of Physical & Occupational Therapy, McGill University, Montreal, Canada (e-mail: philippe.archambault@mcgill.ca).

978-1-4244-4775-6/09/$25.00 © 2009 IEEE.

the dynamic model of the proposed *ExoRob* as well as to evaluate the effectiveness of the controller.

To maneuver the proposed *ExoRob* in manual control scheme [21] as well as to provide *passive mode of rehabilitation,* this paper also focused on the development of a 7DOF upper-limb prototype (lower scaled) master *exoskeleton arm (mExoArm)* which corresponds to the proposed *ExoRob*.

In the next section of this paper, an overview of the development of the kinematical and dynamic model for the proposed *ExoRob* is presented. Details about the controller are explained in section III. In section IV, simulation results are presented to validate the dynamic model as well as to evaluate the performance of the controller. Section V describes the developed *mExoArm* and finally the paper ends with the conclusion in section VI.

II. Kinematical Model

In this study, the proposed *ExoRob* is modeled based on the concept of human upper limb articulations and movement to rehabilitate and to ease shoulder, elbow and wrist joint motion of subjects. To assist human daily activity properly, the exoskeleton should ideally have seven degrees of freedom (7DOF):

- Shoulder abduction/adduction (2DOF, vertical and horizontal flexion/extension),
- Upper arm rotation (1 DOF, internal/external rotation),
- Elbow flexion-extension (1 DOF),
- Forearm pronation-supination (1 DOF), and
- Wrist movement (2DOF, radial/ulnar deviation, and flexion/extension),

Considering the safety of the robot users and to provide effective rehab therapy as well as to assist in performing essential daily activities e.g., eating, grasping, washing the body etc., preliminary studies on anatomical range [17]-[19] of upper limb motion has been done to choose the suitable movable range for the proposed *ExoRob*. The movable range of proposed *ExoRob* is depicted in Fig. 1, and summarized in Table I. Note that for technical simplicity the range of motion of the *ExoRob* is kept to zero degree for shoulder joint extension. This should have minimal impact, as backward movement of the arm past the midline is seldom used in daily activities.

TABLE I
Range of Movement

Types of Motion	Anatomical Range [18]			*ExoRob's* Range
	Source 1	Source 2	Source 3	
		Shoulder Joint		
Flexion	180^0	170^0	180^0	140^0
Extension	50^0	30^0	60^0	0^0
Abduction	180^0	170^0	180^0	140^0
Adduction	50^0	-	-	0^0
Internal rotation	90^0	90^0	90^0	80^0
External rotation	90^0	90^0	60^0-90^0	60^0
		Elbow & Forearm		
Flexion	140^0	140^0	145^0	130^0
Extension	0^0	0^0	5^0-15^0	0^0
Pronation	80^0	90^0	80^0	80^0
Supination	80^0	85^0	90^0	80^0
		Wrist Joint		
Flexion	60^0	90^0	60^0	60^0
Extension	60^0	70^0	50^0	60^0
Radial Deviation	20^0	20^0	20^0	20^0
Ulnar Deviation	30^0	30^0	30^0	30^0

The joint axes of rotation of human upper limb (as well as proposed *ExoRob)* are depicted in Fig. 2. In this model joint 1, 2, and 3 together constitute the glenohumeral joint, commonly known as the shoulder joint, where joint 1 corresponds to horizontal flexion/extension, joint 2 to vertical flexion/extension, and joint 3 to internal/external rotation. Note that, for this exoskeleton robot, the axes of joints 1, 2, and 3 all intersect at a common point. And the axes of joints 4 and 5 are also intersecting at a common

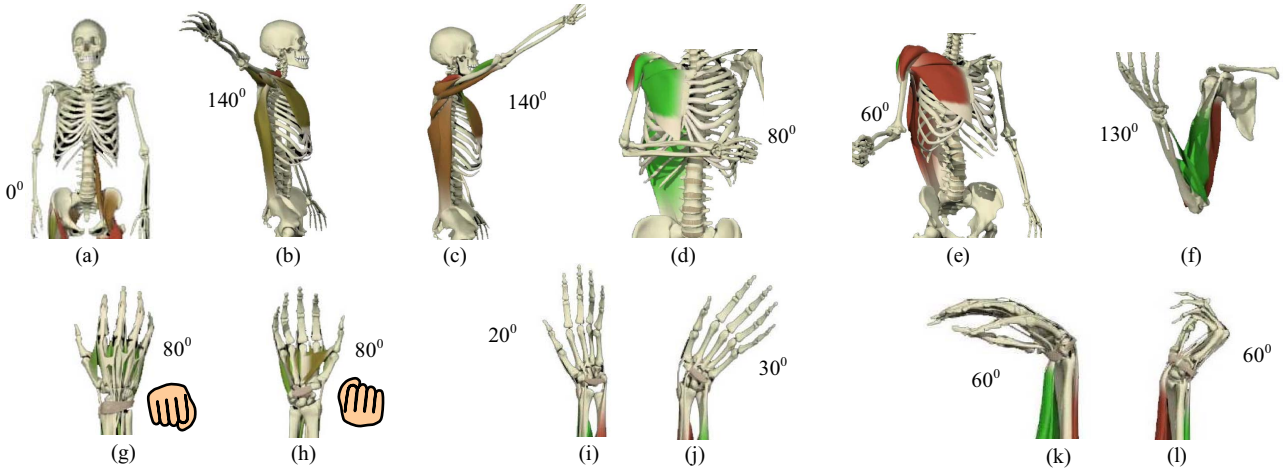

Fig. 1. Movable range of proposed *ExoRob.* (a) Initial (Zero) Position; (b) Shoulder Joint: Abduction, (c) Shoulder Joint: Vertical Flexion; (d) Shoulder Joint: Internal Rotation; (e) Shoulder Joint: External Rotation; (f) Elbow Flexion; (g) Forearm Pronation; (h) Forearm Supination; (i) Radial Deviation; (j) Ulnar Deviation; (k) Wrist Flexion; (l) Wrist Extension

point at a distance d_3 (length of humerus) apart from the glenohumeral joints. It should also be noted that joint 4 corresponds to flexion/extension of elbow joint and joint 5 corresponds to pronation/supination of forearm. As shown in Fig. 2, joints 6 and 7 intersect at another common point known as wrist joint, at a distance d_5 (length of radius) from the elbow joint. For assisting wrist movements, joint 6 corresponds to radial-ulnar deviation and joint 7 to flexion/extension.

To get DH parameters let us assume, the co-ordinate frames (*i.e.,* the link-frames which maps between the successive axes of rotation) are coincide with joint axes of rotation and have the same number of order (*i.e.,* frame {1} coincides with joint 1, frame {2} with joint 2, and so on frame {7} with joint 7) . It is considered that fixed reference frame {0} coincides with the first reference frame (Fig. 2).

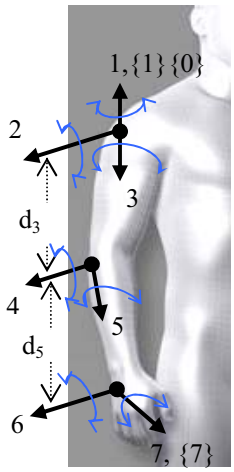

Fig.2. Joint axes of rotation.

We know, the general form of link transformation that relates frame {i} relative to the frame {i-1} [22] is-

$$ {}^{i-1}_{i}T = \begin{bmatrix} c\theta_i & -s\theta_i & 0 & a_{i-1} \\ s\theta_i c\alpha_{i-1} & c\theta_i c\alpha_{i-1} & -s\alpha_{i-1} & -s\alpha_{i-1}d_i \\ s\theta_i s\alpha_{i-1} & c\theta_i s\alpha_{i-1} & c\alpha_{i-1} & c\alpha_{i-1}d_i \\ 0 & 0 & 0 & 1 \end{bmatrix} \quad (1) $$

Using equation (1), the individual homogeneous transfer matrix that relates two successive frame (of Fig. 2) can be written as follows-

$$ {}^{0}_{1}T = \begin{bmatrix} c\theta_1 & -s\theta_1 & 0 & 0 \\ s\theta_1 & c\theta_1 & 0 & 0 \\ 0 & 0 & 1 & 0 \\ 0 & 0 & 0 & 1 \end{bmatrix}, \quad {}^{1}_{2}T = \begin{bmatrix} c\theta_2 & -s\theta_2 & 0 & 0 \\ 0 & 0 & 1 & 0 \\ -s\theta_2 & -c\theta_2 & 0 & 0 \\ 0 & 0 & 0 & 1 \end{bmatrix} $$

$$ {}^{2}_{3}T = \begin{bmatrix} c\theta_3 & -s\theta_3 & 0 & 0 \\ 0 & 0 & -1 & 0 \\ s\theta_3 & c\theta_3 & 0 & 0 \\ 0 & 0 & 0 & 1 \end{bmatrix}, \quad {}^{3}_{4}T = \begin{bmatrix} c\theta_4 & -s\theta_4 & 0 & 0 \\ 0 & 0 & 1 & 0 \\ -s\theta_4 & -c\theta_4 & 0 & d_3 \\ 0 & 0 & 0 & 1 \end{bmatrix} $$

$$ {}^{4}_{5}T = \begin{bmatrix} c\theta_5 & -s\theta_5 & 0 & 0 \\ 0 & 0 & -1 & 0 \\ s\theta_5 & c\theta_5 & 0 & 0 \\ 0 & 0 & 0 & 1 \end{bmatrix}, {}^{5}_{6}T = \begin{bmatrix} c\theta_6 & -s\theta_6 & 0 & 0 \\ 0 & 0 & 1 & 0 \\ -s\theta_6 & -c\theta_6 & 0 & d_5 \\ 0 & 0 & 0 & 1 \end{bmatrix} $$

$$ {}^{6}_{7}T = \begin{bmatrix} 0 & 0 & 1 & 0 \\ -s\theta_7 & -c\theta_7 & 0 & 0 \\ c\theta_7 & -s\theta_7 & 0 & 0 \\ 0 & 0 & 0 & 1 \end{bmatrix} \quad (2) $$

The homogenous transformation matrix that relates frame {7} to frame {0} can be obtained by multiplying individual transformation matrices.

$$ {}^{0}_{7}T = {}^{0}_{1}T \cdot {}^{1}_{2}T \cdot {}^{2}_{3}T \cdot {}^{3}_{4}T \cdot {}^{4}_{5}T \cdot {}^{5}_{6}T \cdot {}^{6}_{7}T \quad (3) $$

The single transformation matrix thus found from equation (3) represents the positions and orientations of the reference frame attached to wrist joint (axis 7) regard to the fixed reference frame.

III. Inverse Kinematics and Control

3.1 Inverse Kinematics: The inverse kinematics solution for a manipulator is computationally costly compare to forward kinematics. Moreover, an inverse kinematics problem for a redundant manipulator (manipulator having more than 6DOF) is much more complex since it gives multiple solutions for a specific task. Inverse kinematic solution of the proposed 7DOF *ExoRob* can be obtained by introducing a Jacobian matrix which relates the end-effector Cartesian velocities to the joints angular velocity vector [3].

$$ \dot{X} = J(\theta)\dot{\theta} \quad (4) $$

A solution of this equation is:

$$ \dot{\theta} = J^{+}\dot{X} + (J^{+}J - I)\xi \quad (5) $$

where, $\theta \in \Re^n$, is the joint space vector; $J(\theta)$ is the Jacobian matix with dimension $m \times n$; and $J^{+} = J^{T}(JJ^{T})^{-1}$ is the pseudo inverse generalized and $\xi \in \Re^n$ is an arbitrary vector. It can be fixed in order to take into consideration the internal motion of the robot such that to avoid obstacles, to avoid exceeding its physical limits and to prevent the robot colliding with its own base [4].

3.2 Control: The dynamic behaviour of the *ExoRob*, can be expressed by the following equation [22].

$$ M(\theta)\cdot\ddot{\theta} + V(\theta,\dot{\theta}) + G(\theta) = \tau_{Joints} \quad (6) $$

where, θ is the joint variables vector, τ_{Joints} is the generalized torques vector, $M(\theta)$ is the inertia matrix, $V(\theta,\dot{\theta})$ is the coriolis/centripetal vector, $G(\theta)$ is the gravity vector.

In this paper, we apply a basic nonlinear computed torque control technique [22] to trajectory tracking of the developed

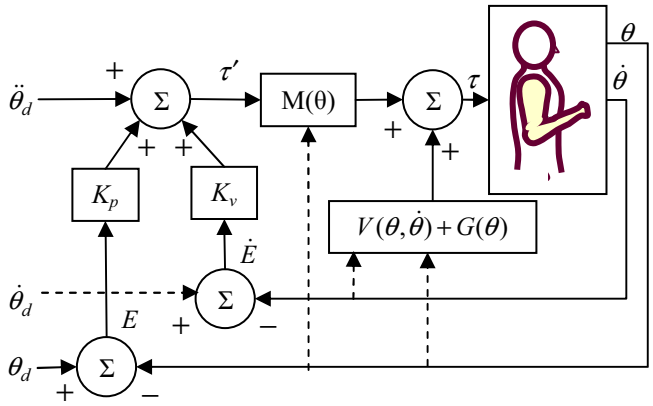

Fig. 3. Schematic Diagram of Computed Torque Control

ExoRob model. The general lay out of the computed torque control technique is depicted in Fig. 3. The control torque in Fig. 3 can be written as:

$$\tau = M(\theta)\left[\ddot{\theta}_d + K_v(\dot{\theta}_d - \dot{\theta}) + K_p(\theta_d - \theta)\right] + V(\theta,\dot{\theta}) + G(\theta) \quad (7)$$

From relations (6) and (7), we may write,

$$\ddot{\theta} = \ddot{\theta}_d + K_v(\dot{\theta}_d - \dot{\theta}) + K_p(\theta_d - \theta) \quad (8)$$

where, $\theta_d, \dot{\theta}_d$, and $\ddot{\theta}_d$ are the desired position, velocity and acceleration respectively and K_p and K_v diagonal positive definite matrices.

Let the error vector E and its derivative be:

$$E = \theta_d - \theta; \quad \dot{E} = \dot{\theta}_d - \dot{\theta}; \quad \ddot{E} = \ddot{\theta}_d - \ddot{\theta} \quad (9)$$

Therefore, equation (8) can be rewritten in the following form:

$$\ddot{E} + K_v\dot{E} + K_pE = 0 \quad (10)$$

K_p and K_v are positive definite matrices, therefore it is very easy to show that the control system is stable.

IV. Simulation

To produce dynamic simulations, *ExoRob* parametes such as masses of different link segments and inertia parameters, are estimated according to the upper limb properties of a typical adult. Table III and IV show the mass and inertial

TABLE III
Mass Characteristics of Upper Limb [15]

Limb Segment	Segment length / Stature	Segment weight/ Body weight	Centre of Mass/ Segment length	Radius of Gyration/ Segment length
			(Proximal)	*(C of G)*
Upper arm [a]	0.186	0.028	0.436	0.322
Forearm [b]	0.146	0.016	0.430	0.303
Hand [c]	0.108	0.006	0.506	0.297
F'arm & Hand	0.254	0.022	0.682	0.468
Upper Limb	0.44	0.050	0.53	0.368

[a] Glenohumeral joint / Elbow , [b] Elbow / Ulnar styloid
[c] Wrist / Knuckle II middle

TABLE IV
Regression Coefficients For Inertia Characteristics of Upper Limb [16]

Limb Segment	Constant	Body Weight (kg)	Stature (cm)	R
Moment of Inertia around X axis [1] (kg.cm^2)				
Upper arm	-250.70	1.56	1.512	0.62
Forearm	-64.00	0.95	0.340	0.71
Hand	-19.50	0.17	0.116	0.50
Moment of Inertia around Y axis (kg.cm^2)				
Upper arm	-232.00	1.525	1.343	0.62
Forearm	-67.90	0.855	0.376	0.71
Hand	-13.68	0.088	0.092	0.43
Moment of Inertia around Z axis (kg.cm^2)				
Upper arm	-16.90	0.6620	0.0435	0.44
Forearm	5.66	0.3060	-0.0880	0.66
Hand	-6.26	0.0762	0.0347	0.43

The origin of the coordinate system for each segment is the center of gravity of that segment. The X axis is defined as the frontal plane and +X is the direction from origin towards the front of the body. The Y axis is defined as the saggital plane and +Y is the direction from the origin towards the left of the body. The Z axis is defined as the transverse plane and +Z is direction from the origin towards the head.

[1] Ex.: Moment of Inertia of hand around X axis (kg.cm^2)= -19.5 + 0.17×Body weight(kg) +0.116×Stature(cm)

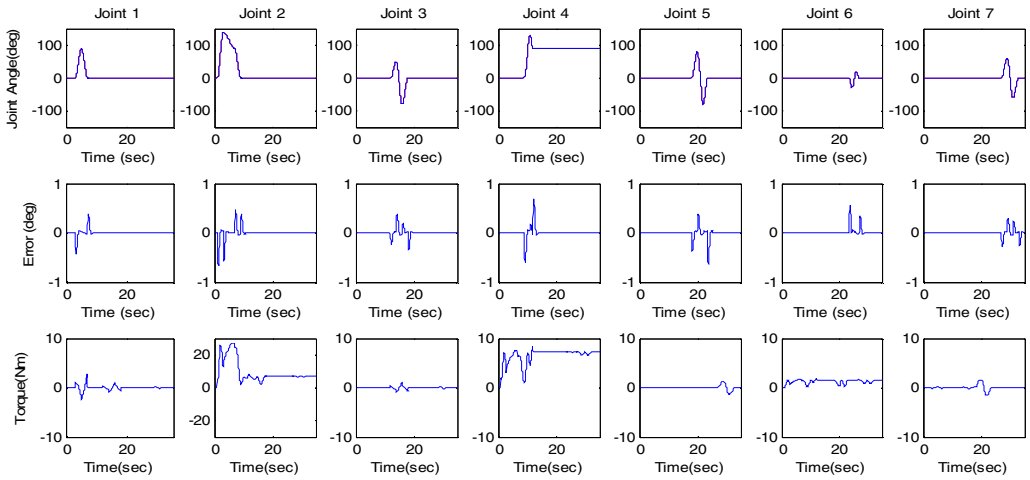

Fig. 4. Trajectory tracking in full range of *ExoRob's* joint's motion

characteristics of a human upper limb used in simulation. Simulations were carried out in the SIMULINK environment (The Mathworks, USA).

Figure 4 shows the results of the simulation that was performed to highlight the tracking performance of the developed controller during full range of motion (i.e., reachable workspace) of the proposed *ExoRob*. The top most plots of Fig. 4 compares the desired joint angles also known as desired trajectories to measured joint angles also known as measured trajectories. It is obvious from the figure that the controller's performance is excellent since measured trajectories completely overlapped with the desired trajectories. Intermediate plots of Fig. 4 show the error as a function of time (i.e., deviation between desired and measured trajectories). It is also obvious from these plots that the error was quite small since it lies below and/or near around 0.5°. Generated joint torques corresponding to the trajectory is plotted in the bottom row.

A simulation of a typical rehabilitation exercise involving motion of the elbow and forearm is depicted in Fig. 5. The objective of this task is to supinate the forearm from the initial position of forearm (Fig. 1a) to the fully supinated position (Fig. 1h), while simultaneously flexing the elbow from complete extension to complete flexion (Fig. 1f) and next, inversely move the forearm from full supination to full pronation position (Fig. 1g), while the elbow simultaneously goes from the complete flexion to extension. Controller tracking performance is certainly obvious from this figure since the desired and measured trajectories also in this case completely overlapped and the deviation was well below 0.25°.

To further evaluate the performance of the controller another desired trajectory, describing a *'repetitive movement of upper-limb over the surface of a table*' (most commonly used occupational therapy) was generated. Figure 6 depicts the tracking performance of the controller for the aforementioned trajectory. Like previous tracking simulation, Fig. 6 also demonstrates the good performance of the controller, with error limited to less than 0.25°.

For the full range of motion (as depicted in Fig. 4) the

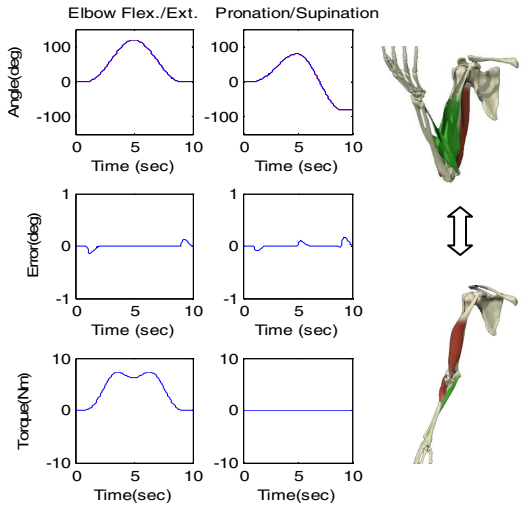

Fig. 5. Elbow and Forearm Motion, Typical Rehab Exercise

maximum tracking deviation is observed at the level of shoulder flexion/extension, which was below 0.5 degree (i.e., tracking error is 0.36% of the total range). For the typical rehab exercises and the occupational therapy (as shown in Fig. 5 and 6), the maximum tracking deviation was well below 0.25 degree (i.e., maximum tracking error is 0.16%). Comparing the natural variability of human arm movement [23]-[28] with these results, we may conclude that the developed model and the controller can efficiently track the desired trajectories, and thus should be adequate for the purpose of performing passive arm movement therapy.

Simulation results thus validate the developed model and also evaluate the performance of the computed torque control technique regard to trajectory tracking.

V. Master Exoskeleton Arm

The *master exoskeleton arm (mExoArm)* as shown in Fig. 7 is developed to maneuver the proposed *ExoRob* in manual control mode as well as to provide *passive mode of*

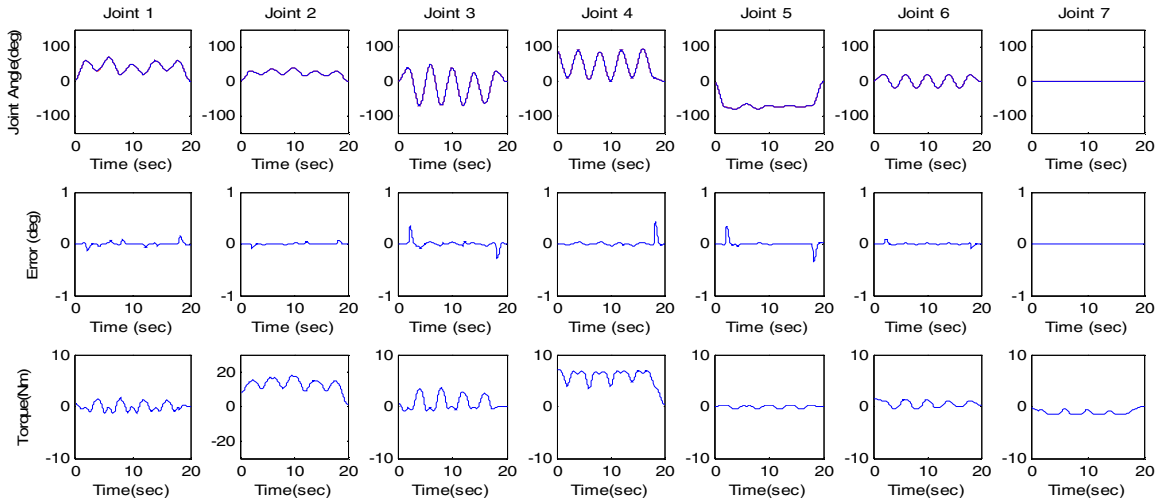

Fig. 6. Trajectory tracking of commonly used occupational exercise. Trajectory describes a repetitive movement of upper -limb over the surface of a table while performing a basic cleaning task.

rehabilitation. The entire *mExoArm* is constructed with ABS (Acrylonitrile butadiene styrene) by rapid prototyping except the base which is made of Aluminum (Fig.7c). As depicted in figure 7, in every joint potentiometer is incorporated with the arm link to give the desired rotational movement of the joints as well as to measure the angle of rotation. Respecting safety issue and anatomical joint movement (Table I) of human upper-limb, we have added mechanical stoppers in every rotational joint in design of *mExoArm* so that it strictly obeys *ExoRob's* range of movement (last column of Table I).

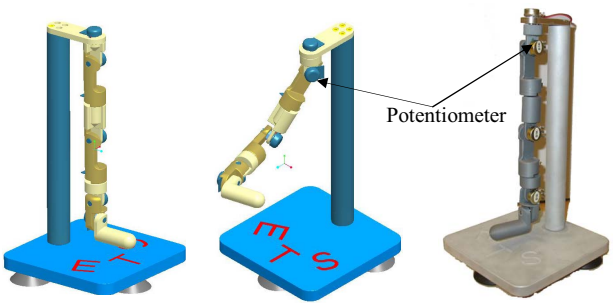

Fig.7. A 7DOF Upper-limb prototype *mExoArm.* (a) Left-front View (Initial Position), (b) Joint 1,2 are rotated to 30^0, Joint 3 is to 60^0 and Joint 4 is to70^0, (c) *mExoArm* after fabrication

VI. Conclusion And Future Works

The kinematical and dynamic model of an exoskeleton robot is presented as a first step toward the building of a 7DOF exoskeleton robot for rehabilitation and to assist upper-limb motion in physically disabled individuals. The nonlinear computed torque control technique was employed in a dynamic simulation of the developed model. Trajectory tracking performance of the controller was evaluated through simulation which in this case consisted in passive arm movements. Such movements are used in physical therapy and could be performed efficiently with the developed model and the controller. An upper-limb prototype 7DOF *master exoskeleton arm (mExoArm)* is developed to maneuver the proposed *ExoRob* in manual control mode as well as to provide *passive mode of rehabilitation*.

Future works will include the design, and development of proposed *ExoRob* based on its kinematical modeling. The proposed *ExoRob* will be worn to the lateral side of patient's upper limb and will be controlled in real time by the skin surface electromyogram (EMG) signals, since EMG signals directly reflect a user's intention of motion [21].

References

[1] https://www.cia.gov/library/publications/the-world-factbook/#People

[2] A Portrait of Seniors in Canada 2006: Catalogue no. 89-519-XIE20, www.statcan.ca.

[3] D.E. Whitney, "Resolved motion rate control of manipulators and human prostheses," *IEEE Trans. on Man-Machine Systems*, vol. 10, no. 2, pp. 47-53, 1969.

[4] B. LeBoudec, M. Saad, and V. Nerguizian, "Modeling and Adaptive Control of Redundant Robots", *Mathematics and Computers in Simulation,* vol. 71, no. 4-6, pp. 395-403, June 2006.

[5] N.G. Tsagarkis, D.G. Caldwell, "Development and Control of a "Soft-Actuated Exoskeleton for use in Physiotherapy and Training," *Autonomous Robots,* pp. 15-21, 2003.

[6] M.L. Moe, J.T. Shwartz, Ocular Control of the Rancho Electric Arm, Advances in External Control of Human Extremities, Belgrade, 1973.

[7] P.H. Stern, T. Lauko. "Modular Designed, Wheelchair based Orthotic System for Upper Extremities," *Paraplegia,* vol. 12, pp. 299-304, 1975.

[8] N. Benjuya, S.B. Kenney, "Hybrid arm orthosis," *Journal of Prosthetics and Orthotics,* vol. 2, no. 2, pp. 155–163, 1990.

[9] H.I. Kerbs, B.T. Volpe, M.L. Aisen, N. Hogan, "Increasing Productivity and Quality of Care: Robot-aided neuro-rehabilitation," *Journal of Rehabilitation Research and Development*, vol. 37, no. 6, pp. 639-652, 2000.

[10] H.I. Krebs, N. Hogan, M.L. Aisen, B.T. Volpe, "Robot aided Neuro-Rehabilitation," *IEEE Trans. on Rehabilitation Eng.,* pp. 75–87, 1998.

[11] M.A. Alexander, M.R. Nelson, A. Shah, Orthotics, Adapted Seating and Assistive Devices, Pediatric Rehabilitation 2nd ed . Baltimore MD: Williams and Wilkins, pp. 186-187, 1992.

[12] K. Homma, T. Arai., "Design of an Upper Limb Assist System with Parallel Mechanism," *IEEE International Conference on Robotics and Automation,* pp. 1302–1307, 1995.

[13] D.J. Reinkensmeyer, J.P.A. Dewald, W.Z. Rymer, "Guidance-Based Quantification of Arm Impairment Following Brain Injury", *IEEE Trans. on Rehabilitation Eng.,* vol. 7, no. 1, pp. 1-11, 1999.

[14] C.G. Burgar, P.S. Lum, P.C. Shor, and H.F.V.d.L. Machiel, "Development of Robots for Rehabilitation Therapy: The Palo Alto VA/Stanford Experience," *Journal of Rehabilitation Research and Development,* vol. 37, no. 6, pp. 663-673, 2000.

[15] A.D. Winter, Biomechanics and Motor Control of Human Movements, 2nd ed., University of Waterloo Press, Canada,1992.

[16] V. Zatsiorsky, and V. Seluyanov, "The Mass and Inertia Characteristics of the Main Segments of the Human Body," Biomechanics VIII-B, University Park Press, pp. 1152-1 159, 1983.

[17] Gray, Henry, Anatomy of the Human Body, Philadelphia: Lea & Febiger, 1918; Bartleby.com, 2000, ISBN: 1-58734-102-6.

[18] http://www.bsu.edu/web/ykwon/pep294/lab2/rom_lab.html

[19] S.K. Hillman, Interactive Functional Anatomy-DVD, Primal Pictures Ltd., London, 2003.

[20] J. Rosen, C. Perry, N. Manning, S. Burns, B. Hannaford, "The Human Arm Kinematics and Dynamics During Daily Activities – Toward a 7 DOF Upper Limb Powered Exoskeleton," *ICAR 2005,* Seattle WA, July 2005.

[21] K. Kiguchi, M.H. Rahman, and M. Sasaki, "Neuro-Fuzzy based Motion Control of a Robotic Exoskeleton: Considering End-effector Force Vectors," *IEEE International Conference on Robotics and Automation* , pp. 3146-3151, USA, May, 2006.

[22] J.J. Craig, Introduction to Robotics: Mechanics and Control, 2nd Edition, Addison-Wesley, New York, 1989.

[23] H. Laurette, B. Chantal, F. Carole, O. Isabelle, and F. Michelle, "Role of proprioceptive information in movement programming and control in 5 to 11-year old children," *Human Movement Science*, vol. 24, no.2, pp.139-154, 2005.

[24] T.D. Sanger, "Human Arm Movements Described by a Low-Dimensional Superposition of Principal Components," *The Journal of Neuroscience*, vol. 20, no. 3, pp. 1066-1072, Feb., 2000.

[25] R.J.v. Beers, P. Haggard, and D.M. Wolpert, "The Role of Execution Noise in Movement Variability," *Journal of Neurophysiology*, vol. 91, pp.1050-1063, Feb. 2004.

[26] D.E. Meyer, R.A. Abrams, S. Kornblum, C.E. Wright, and J.E.K. Smith, "Optimality in Human Motor Performance: Ideal Control of Rapid Aimed Movements" *Psychological Review,* vol. 95, no. 3, pp. 340–370, 1988.

[27] C.A. Buneo, J. Boline, J.F. Soechting, and R.E. Poppele, "On the Form of the Internal Model for Reaching," *Experimental Brain Research,* vol. 104, no. 3, pp. 467–479, 1995.

[28] C. Ghez, J. Gordon, M.F. Ghilardi, C.N. Christakos, and S.E. Cooper, "Roles of Proprioceptive Input in the Programming of Arm Trajectories," *Cold Spring Harbor Symposia on Quantitative Biology,* vol. 55, pp. 837–847, 1990.